# Conformal Micropatterned Organic-Metal Electrodes for Physiological Recording

Kirstie M. Queener[1,2], Parvez Ahmmed[1], Mauro Victorio[3], Jack Twiddy[1,2], Ashley Dehn[1,2], Alec Brewer[1], Edgar Lobaton[1], Alper Bozkurt[1], Vladimir Pozdin[3] and Michael Daniele[1,2]

[1]North Carolina State University, Raleigh, NC USA
[2]University of North Carolina at Chapel Hill, Chapel Hill, NC USA
[3]Florida International University, Miami, FL USA
E-mail: mdaniel6@ncsu.edu, aybozkur@ncsu.edu, vpozdin@fiu.edu, ejlobato@ncsu.edu

***Abstract*— Conformal electrodes provide a soft and conforming interface with the skin for reduced impedance, comfortable skin contact, and improved signal quality compared to commercial electrodes. In this paper, we present conformal micropatterned organic-metal (CMOM) electrodes and our investigation on the effect of perforation micropatterning and PEDOT:PSS coating. CMOM electrodes were characterized then evaluated *in vivo* against commercial-off-the-shelf electrodes. PEDOT:PSS was found to reduce the overall impedance in each electrode variant, resulting in a >97% decrease in impedance at low frequencies. The change in impedance at high frequencies was not significant for the control or 30 µm vias electrodes, but the impedance was significantly greater following EPD for 60 µm vias electrodes.**

***Keywords—conformal electrodes; biopotential recording; microfabrication; photolithography; PEDOT:PSS***

## I. Introduction

Commercial Ag/AgCl gel electrodes are the standard for recording biopotential signals. These "wet" electrodes provide a non-polarizable interface with low contact impedance and high conductivity. This reduces motion artifacts and increases the transduced magnitude of the signal [1-3]. However, the gel may irritate the skin by maceration, and electrode displacement and property changes during drying causes performance drift [2, 4, 5]. Dry electrodes, on the other hand, interface with the skin via mechanical coupling of inert conducting material and the skin without the need for the gel. Dry electrodes are typically made of polarizable materials, *e.g.,* gold and stainless steel. As no gel is used, signals recorded from dry electrodes can have higher contact impedance and signal instability due to motion artifacts [1-3]; however, the extended use of dry electrodes for longitudinal recording is more viable [3, 5].

Multiple dry electrode designs have been reported [2, 4, 6, 7] to overcome high contact impedance and motion artifact issues, of which, the most popular ones are conformal, thin-film designs [2, 4, 7, 8]. In terms of mechanical properties, conformal electrodes are thin and soft, which allows them to couple with a wide range of skin curvatures, enabling recordings in various body locations. Their closer contact with the skin brings the potential of eliminating additional gel material and reduces the overall thickness. This enables improved compatibility with hairy skin and sustained adhesion in wet environments [8]. These interface advantages also allow for a reduction in motion artifact, when compared to standard electrodes for longer-term monitoring with high signal quality [4].

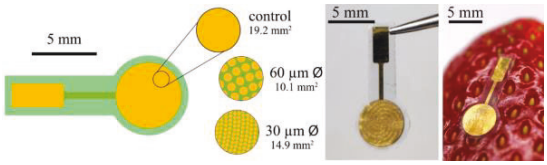


Fig. 1. Schematic of fabricated electrode variants with microperforations and photographs of final conformable electrode.

Conformal electrodes are commonly demonstrated for electrophysiological and soft electronics applications, enabled by the ability to realize highly flexible substrates and conductors by reducing material thickness and tuning conductor geometry [9-11]. More recently, novel conductors and designs have been used to engineer tattoo-like electrodes for recording electrocardiograms (ECG), surface electromyograms, and seismocardiograms [2, 7]. An emerging design is the direct printing of conductive inks onto carrier substrates [12] or even human skin [13]. These examples have been used to measure pressure, temperature, and moisture levels. While conformal electrodes show promise, additional work is needed to realize commercial and clinical viability. Specifically, fabrication process and reliability of conformal electrodes require improvement.

Herein, we report the fabrication, electrical characterization, and *in vivo* performance of a new electrode type: conformal micropatterned organic-metal (CMOM) electrodes (see Fig. 1). CMOM electrodes are soft electrodes that conform to the skin, which allows for improved signal quality and reduced impedance. Micropatterning of CMOM electrodes allows for specific introduction of conductive polymers, such as poly(3,4-ethylenedioxythiophene) polystyrene sulfonate (PEDOT:PSS), which reduce interfacial impedance, motion artifacts, and are particularly biocompatible in skin-worn and sweaty conditions [8, 14, 15]. We investigated the effect of micropatterning the insulation layer, with regard to both electrode characteristics and the ultimate effect of the electropolymerization deposition (EPD) of PEDOT:PSS. We demonstrated the integration and performance of CMOM electrodes with a wearable device for physiological recording.

This work was supported by the U.S. National Science Foundation (IIS-2037328, ECCS-2231012) and through an Nanosystems Engineering Research Center for Advanced Self-Powered Systems for Integrate Sensors and Technologies (EEC-1160483). This work was performed in part at the Analytical Instrumentation Facility at North Carolina State University.

2023 IEEE SENSORS | 979-8-3503-0387-2/23/$31.00 ©2023 IEEE | DOI: 10.1109/SENSORS56945.2023.10324963

## II. Materials & Methods

### A. Fabrication of Electrodes

Briefly, 38 µm thick PET sheets were laminated onto polydimethylsiloxane (PDMS, Sylgard™ 184) coated soda lime glass wafers. A Cr/Au (30/100 nm) metallization layer was deposited by e-beam physical vapor deposition. Standard AZ1518 process on a mask aligner (MA6/BA6, SÜSS MicroTec SE) was used to create an electroplating mask. Gold was electroplated using TSG-250 solution under constant 3.5 mA/cm$^2$ at 60 °C for 60 s to decrease resistance of electrode traces. The final metal trace thickness was 200-250 nm. After electroplating, the AZ1518 process was used to define a wet etch mask to remove the seed Cr/Au layers and define electrode shape. The wafer was coated with Parylene-C (2.2 µm) using adhesion promoter (Silane A174, MilliporeSigma). Standard AZ4680 process was used to define a dry etch mask for electrical connections and active electrode area. Parylene-C was selectively etched using $O_2$/Ar plasma (PlasmaTherm 790). Selective Parylene-C etching served to create three different variants in electrode design. After mask removal, CMOM electrodes were cut out with a $CO_2$ laser (Versa 3.60, Universal Laser Systems).

PEDOT:PSS was deposited on the electrodes by EPD. The aqueous EPD solution was 3,4-ethylenedioxythiophene (EDOT) and poly(sodium 4-styrene sulfonate), 0.1M and 1% w/v, respectively. Prior to EPD, electrodes were cleaned in 1:1 EtOH:DI water. EPD was conducted by chronopotentiometry using a potentiostat/galvanostat (PGSTAT128N, Metrohm Autolab BV) in galvanostatic mode. Current was duty cycled at 0 mA for 5 s followed by 3.29 mA for 30 s. The applied current was determined to achieve a current density of 0.02 nA/µm$^2$ [14, 15], assuming a planar geometric surface area.

Each electrode variant was imaged prior to and following EPD. Brightfield and scanning electron micrographs are shown in Fig. 2. All SEM imaging samples were sputter coated with Au-Pd (20 nm) for improved electron microscopy and images were taken at a 20° angle at 20 kV.

### B. Electrical Characterization

Each electrode variant was characterized by electrical impedance spectroscopy (EIS) from 1 Hz - 100 kHz, using the potentiostat/galvanostat (PGSTAT128N, Metrohm Autolab BV). EIS was performed in galvanostatic mode with a frequency sweep from 100 kHz - 1 Hz, 10 $\mu A_{RMS}$ sine wave, and recorded at 10 frequencies per decade.

### C. Physiological Recordings

Two *in vivo* tests were performed to demonstrate the effectiveness of CMOM electrodes for electrophysiological recording and biometric monitoring. The recording device was a custom-designed wearable chest patch with a Bluetooth™ enabled microcontroller (CC2642, Texas Instruments), a bioelectrophotonic front-end circuit (AFE4900, Texas Instruments), an impedance spectroscopy front-end circuit (AD5941, Analog Devices, Inc.), and a MEMS accelerometer (ADXL362, Analog Devices, Inc.). The experimental procedure was approved by the Institutional Review Board at NC State University. First, three electrode measurements (positive, negative, and right leg drive) were compared using CMOM electrodes with

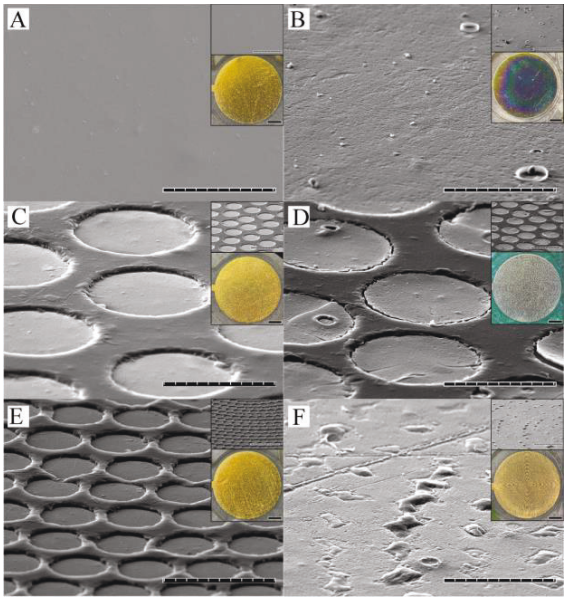


Fig. 2. Electron micrographs and photographs (insets) of CMOM electrode variants 1-3, prior to (A, C, E) and following (B, D, F) EPD of PEDOT:PSS. Electron micrographs: (1000X; scale = 50 µm). Electron micrograph insets: (500X; scale = 100 µm). Photographs: (45X; scale = 1 mm).

PEDOT:PSS coating versus three commercial-off-the-shelf (COTS) electrodes (Red Dot™ 2560, 3M) by attaching electrodes to the resting subject's chest in two separate rows. ECG signals were recorded from both electrode sets simultaneously using two identical recording devices. For the second test, four dry CMOM electrodes were attached horizontally across the chest to the device on the sternum. Simultaneous 4-wire bioimpedance (with 180 kHz excitation current) and tri-axial acceleration were recorded while the subject was performing fast and shallow breathing.

## III. Results & Discussion

### A. Fabrication and Electrical Characterization

Three CMOM electrode variants were fabricated to investigate the effect of perforation on subsequent EPD of PEDOT:PSS and physiological recording. Variant 1, the non-perforated control, was a bare circular electrode with diameter of 5 mm and active surface area of 19.63 mm$^2$. For microperforated variants, Parylene-C encapsulation was selectively etched to form an array of circular vias with diameters of 60 µm or 30 µm, *i.e.,* Variants 2 and 3 with total active surface area of 6.99 mm$^2$ and 6.62 mm$^2$, respectively. The fabrication of 30 µm vias resulted in some vias that were merged, notably towards the center of the electrode (see Fig. 2F). Since the surface area differs among variants, the current required to attain the same current density for each variant was calculated. However, upon EPD for the first Variant 2 electrode, we observed that PEDOT:PSS was not deposited using the current calculated from the current density. EPD for Variant 2 and Variant 3 was carried out using the current calculated for Variant 1.

The Nyquist plots show that EPD of PEDOT:PSS reduces the Faradaic contribution and makes the electrodes more suitable for electrophysiological signal recording (Fig. 3). The Bode plots indicate that PEDOT:PSS reduces the

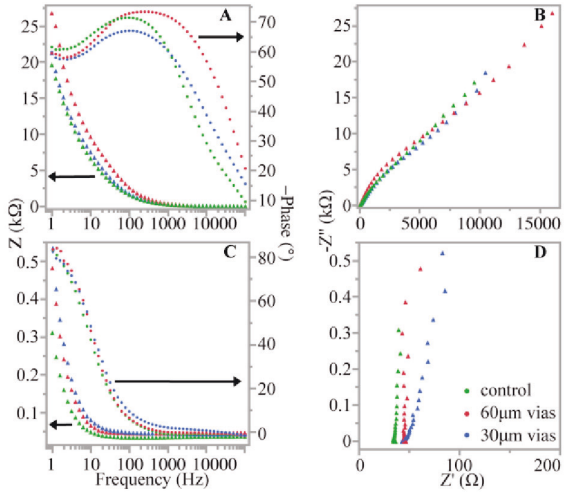


Fig. 3. (A, C) Bode and (B, D) Nyquist plots for CMOM electrodes prior to and following the EPD, respectively. Green points = control, Red points = 60 µm vias, Blue points = 30 µm vias. Points represent data averages (control: $n = 7$, 30 µm: $n = 3$, and 60 µm: $n = 3$).

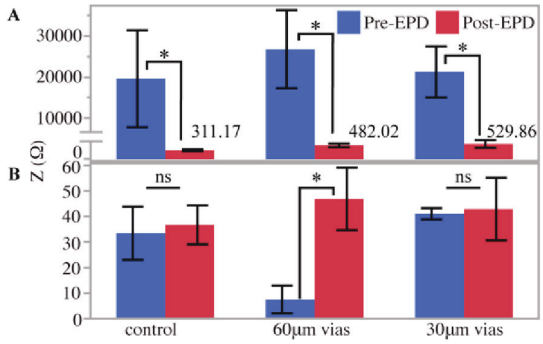


Fig. 4. Bulk impedance for CMOM electrodes at (A) 1 Hz and (B) 100 kHz, (control: $n = 7$, 30 µm: $n = 3$, and 60 µm: $n = 3$). * represents $p < 0.05$ by one-way ANOVA and Tukey-Kramer HSD, $\alpha$=0.05. Error bars are ± 1 S.D.

overall impedance in each electrode variant, especially at low frequencies (Fig. 3). The pre-EPD electrodes with 60 µm vias have the highest impedance as they have the smallest exposed gold area and are more capacitive. Even so, they have a bulk impedance that is comparable to COTS electrodes. Red Dots™ have a bulk impedance of 10-100 kΩ at 1 Hz [16], while pre-EPD impedance was 19.6-26.8 kΩ and post-EPD impedance was 0.3-0.5 kΩ. At high frequencies, the change in impedance was not significant except for the 60 µm vias design, which was significantly increased following EPD (Fig. 4). The change in impedance at high frequencies post-EPD did not follow the expected trend and thus requires additional investigation to understand post-EPD CMOM behavior. However, all variants had lower impedance compared to Red Dots™, which have a bulk impedance of between 1 and 10 kΩ at 1 kHz [16]. All CMOM electrodes had an impedance of <47 Ω at 100 kHz.

### *B. Physiological Recordings*

The first experiment demonstrated the detection of heart rate from biopotential measurements. We realized that CMOM electrodes were not producing discernible ECG peaks due to the deformation from the bulky connections in the benchtop setup. Hence, we used isotonic electrode gel (GEL101, BIOPAC Systems, Inc.) for proof-of-concept

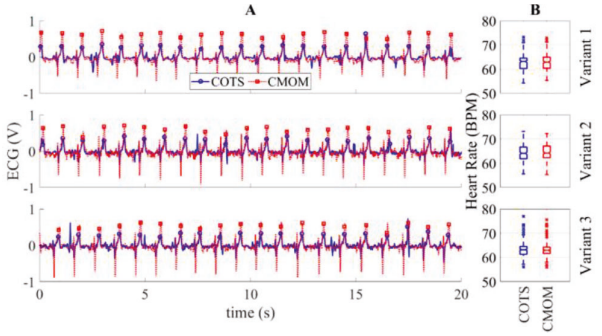


Fig. 5. (A) Three sets of simultaneous ECG signals recorded using the three variants of CMOM electrodes along with COTS electrodes using two identical acquisition devices. (B) Whisker plots showing the median and interquartile range of the extracted heart rate values.

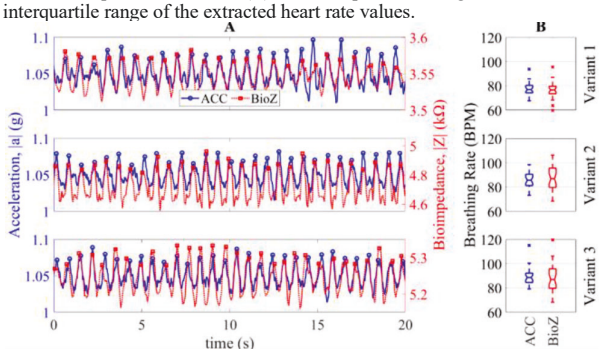


Fig. 6. (A) Simultaneous traces of the magnitude of acceleration (ACC) and bioimpedance (BioZ, with 180 kHz excitation frequency) recorded using the three variants of CMOM electrodes. (B) Whisker plots showing the median and interquartile range of the extracted breathing rate values.

demonstration. Fig. 5A shows the transient ECG plots from the two devices which confirm similar signal quality and synchronization of heart beats. The difference in extracted heart rate values between the COTS and CMOM electrodes for each variant was not significant (Fig. 5B). The second experiment demonstrated the detection of breathing rate from bioimpedance and inertial measurements. Fig. 6 shows the transient plots of breathing artifacts and the statistics of breathing rate values. The difference in breathing rate values extracted from the two sensors was not significant.

## IV. Conclusions & Future Work

In general, conformal electrodes bring many potential advantages over COTS wet and dry electrodes. The high-quality skin-electrode interface, reduction in motion artifacts, and mechanical robustness of conformal electrodes allow them to be used for a variety of health monitoring applications[2, 4, 7, 8]. While the CMOM electrodes that we have developed still require isotonic gel, they are small, thin, and flexible. As such, they could be used in applications such as sleep studies, extended wear monitoring, or even be integrated into other soft electronics. Further development is required to remove the need for isotonic gel, such as the development of conformal circuits boards and interconnects for long-term performance testing to understand the lifetime, impedance characteristics, and durability of CMOM electrodes. The *in vivo* performance will be further investigated to characterize performance during dry operation and subject movement. Finally, more in-depth biocompatibility testing, such as fouling, skin sensitivity, and electrochemical stability, will be evaluated.

## REFERENCES


[1] S. Rajaraman, J. A. Bragg, J. D. Ross, and M. G. Allen, "Micromachined three-dimensional electrode arrays for transcutaneous nerve tracking," *J Micromech Microeng,* vol. 21, no. 8, 2011.

[2] Y. Wang *et al.*, "Electrically compensated, tattoo-like electrodes for epidermal electrophysiology at scale," *Science Advances,* vol. 6, no. 43, p. eabd0996, 2020.

[3] A. Searle and L. Kirkup, "A direct comparison of wet, dry and insulating bioelectric recording electrodes," *Physiological Measurement,* vol. 21, no. 2, p. 271, 2000.

[4] Y. Zhao *et al.*, "Ultra-conformal skin electrodes with synergistically enhanced conductivity for long-time and low-motion artifact epidermal electrophysiology," *Nature Communications,* vol. 12, no. 1, p. 4880, 2021.

[5] H. Kim, E. Kim, C. Choi, and W. H. Yeo, "Advances in Soft and Dry Electrodes for Wearable Health Monitoring Devices," (in eng), *Micromachines (Basel),* vol. 13, no. 4, 2022.

[6] M. F. Hossain, J. S. Heo, J. Nelson, and I. Kim, "Paper-Based Flexible Electrode Using Chemically-Modified Graphene and Functionalized Multiwalled Carbon Nanotube Composites for Electrophysiological Signal Sensing," *Information*, vol. 10, no. 10*,* 2019.

[7] S. Bhattacharya *et al.*, "A Chest-Conformable, Wireless Electro-Mechanical E-Tattoo for Measuring Multiple Cardiac Time Intervals," *Advanced Electronic Materials,* p. 2201284, 2023.

[8] S. Liu, Y. Rao, H. Jang, P. Tan, and N. Lu, "Strategies for body-conformable electronics," *Matter,* vol. 5, no. 4, pp. 1104-1136, 2022.

[9] D.-H. Kim *et al.*, "Epidermal Electronics," *Science,* vol. 333, no. 6044, pp. 838-843, 2011.

[10] D.-H. Kim *et al.*, "Stretchable and Foldable Silicon Integrated Circuits," *Science,* vol. 320, no. 5875, pp. 507-511, 2008.

[11] J. A. Rogers, T. Someya, and Y. Huang, "Materials and Mechanics for Stretchable Electronics," *Science,* vol. 327, no. 5973, pp. 1603-1607, 2010.

[12] M. K. Kim *et al.*, "Soft-packaged sensory glove system for human-like natural interaction and control of prosthetic hands," *NPG Asia Materials,* vol. 11, no. 1, p. 43, 2019.

[13] N. X. Williams, S. Noyce, J. A. Cardenas, M. Catenacci, B. J. Wiley, and A. D. Franklin, "Silver nanowire inks for direct-write electronic tattoo applications," (in eng), *Nanoscale,* vol. 11, no. 30, pp. 14294-14302, 2019.

[14] P. D. Jones *et al.*, "Low-Impedance 3D PEDOT:PSS Ultramicroelectrodes," (in English), *Frontiers in Neuroscience,* Original Research vol. 14, 2020.

[15] R. Gerwig *et al.*, "PEDOT–CNT Composite Microelectrodes for Recording and Electrostimulation Applications: Fabrication, Morphology, and Electrical Properties," *Frontiers in Neuroengineering,* Original Research vol. 5, 2012.

[16] B. M. Li, O. Yildiz, A. C. Mills, T. J. Flewwellin, P. D. Bradford, and J. S. Jur, "Iron-on carbon nanotube (CNT) thin films for biosensing E-Textile applications," *Carbon,* vol. 168, pp. 673-683, 2020.